Pergamon

Cement and Concrete Research 30 (2000) 1289–1294

CEMENT AND CONCRETE RESEARCH

Communication

Uniaxial tension in carbon fiber reinforced cement, sensed by electrical resistivity measurement in longitudinal and transverse directions

Sihai Wen, D.D.L. Chung*

Composite Materials Research Laboratory, Department of Mechanical and Aerospace Engineering, State University of New York at Buffalo, Buffalo, NY 14260-4400, USA

Received 19 November 1999; accepted 4 May 2000

Abstract

Uniaxial tension of carbon fiber reinforced cement paste in the elastic regime caused reversible increases in both longitudinal and transverse resistivities. Without the fibers, the resistivity increase was much smaller and less reversible. © 2000 Elsevier Science Ltd. All rights reserved.

Keywords: Electrical properties; Strain effect; Cement paste; Microcracking; Carbon fibers

1. Introduction

Cement reinforced with short carbon fibers is capable of sensing its own strain due to the effect of strain on the electrical resistivity [1–12]. As observed at 28 days of curing, the resistivity in the stress direction increases upon tension, due to slight fiber pull-out that accompanies crack opening, and decreases upon compression, due to slight fiber push-in that accompanies crack closing [6–11]. However, little attention has been previously paid to the resistivity in directions other than the stress direction. In practical use of carbon fiber reinforced cement for strain sensing, the resistivity is not necessarily measured in the stress direction. Furthermore, how the resistivity changes in directions other than the stress direction provides valuable insight on the mechanism behind the piezoresistive effect. Therefore, for both technological and scientific reasons, it is important to investigate the resistivity in directions other than the stress direction. For simplicity, this article is focused on the resistivity in the transverse direction (i.e., a direction perpendicular to the stress axis) for the case of uniaxial tension. However, for the sake of comparison, investigation was also conducted in this work for the resistivity in the longitudinal direction. Moreover, resistivities in both longitudinal and transverse directions were measured for cement with and without carbon fibers in order to study the effect of the fibers.

2. Experimental methods

The carbon fibers were isotropic pitch-based and unsized, as obtained from Ashland Petroleum (Ashland, KY). The fiber diameter was 15 μm. The nominal fiber length was 5 mm. Fibers in the amount of 0.5% by mass of cement were used. Prior to using the fibers in the cement, they were dried at 110°C in air for 1 h and then surface-treated with ozone by exposure to O_3 gas (0.6 vol.%, in O_2) at 160°C for 10 min. The ozone treatment was for improving the wettability of fibers by water [10]. The cement used was Portland cement (Type I) from Lafarge (Southfield, MI). The silica fume (Elkem Materials, Pittsburgh, PA, microsilica, EMS 965) was used in the amount of 15% by mass of cement. The methylcellulose, used in the amount of 0.4% by mass of cement, was from Dow Chemical, Midland, MI, Methocel A15-LV. The defoamer (Colloids, Marietta, GA, 1010) used whenever methylcellulose was used was in the amount of 0.13 vol.% (% of sample volume). The latex, used in the amount of 20% by mass of cement, was styrene butadiene copolymer (Dow Chemical, Midland, MI, 460NA) with the polymer making up about 48% of the dispersion and with styrene and butadiene in the mass ratio 66:34, such that the

* Corresponding author. Tel.: +1-716-645-2593 ext. 2243; fax: +1-716-645-3875.

E-mail address: ddlchung@acsu.buffalo.edu (D.D.L. Chung).

PII: S0008-8846(00)00304-5

latex was used along with an antifoam (Dow Corning, Midland, MI, #2410, 0.5% by mass of latex).

A rotary mixer with a flat beater was used for mixing. Methylcellulose (if applicable) was dissolved in water and then the defoamer (if applicable) and fibers (if applicable) were added and stirred by hand for about 2 min. Latex (if applicable) was mixed with the antifoam agent and fibers (if applicable) by hand for about 1 min. The methylcellulose mixture (if applicable), the latex mixture (if applicable), cement, water, silica fume (if applicable) were mixed in the mixer for 5 min. After pouring the mix into oiled molds, an external electric vibrator was used to facilitate compaction and decrease the amount of air bubbles. The specimens were demolded after 1 day and then allowed to cure at room temperature in air (relative humidity=100%) for 28 days.

Fiber types of cement paste were studied, namely (i) plain cement paste (consisting of just cement and water), (ii) silica-fume cement paste (consisting of cement, water and silica fume), (iii) carbon-fiber silica-fume cement paste (consisting of cement, water, silica fume, methylcellulose, defoamer and carbon fibers), (iv) latex cement paste (consisting of cement, water, latex, carbon fibers and antifoam agent), and (v) carbon-fiber latex cement paste (consisting of cement, water, latex, carbon fibers and antifoam agent). The water/cement ratio was 0.35 for pastes (i), (ii) and (iii), and was 0.23 for pastes (iv) and (v). Six specimens of each of the five types of paste were tested.

Dog-bone-shaped specimens of the dimensions shown in Fig. 1(a) were used for tensile testing. The specimen cross-section was 30 × 20 mm in the narrow part of the dog-bone shape. They were prepared by using molds of the same shape and size. Tensile testing was performed using a Sintech 2/D screw-action mechanical testing system under repeated loading at various stress magnitudes, which corresponded to load amplitudes of 10, 20 and 30 lb (i.e., 0.45, 0.91, and 1.36 kg, respectively). The loading speed was 0.5 mm/min.

During tensile testing, both longitudinal and transverse strains were measured by using strain gages attached to the centers of the opposite sides at the narrow part of the dog-bone-shaped specimen (Fig. 1(b)). Simultaneously with mechanical testing, DC electrical resistance was measured using the four-probe method. The longitudinal and transverse resistances were measured along the stress axis and in the direction perpendicular to the stress axis, respectively.

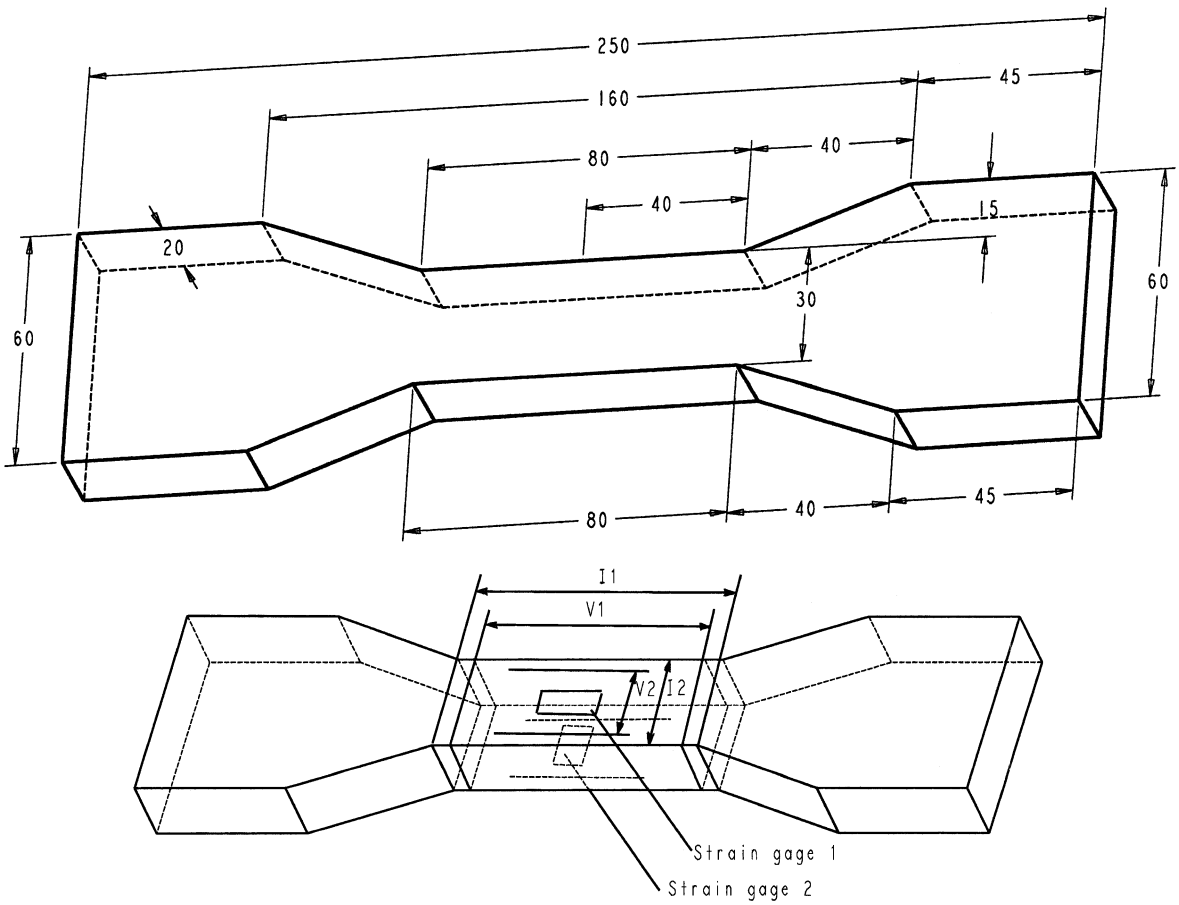

Fig. 1. Specimen configuration. (a) Dimensions are in millimeters. (b) I1 and V1 indicate current and voltage contacts, respectively, for longitudinal resistance measurement. I2 and V2 indicate current and voltage contacts, respectively, for transverse resistance measurement. Strain gages 1 and 2 are for measuring the longitudinal and transverse strains, respectively.

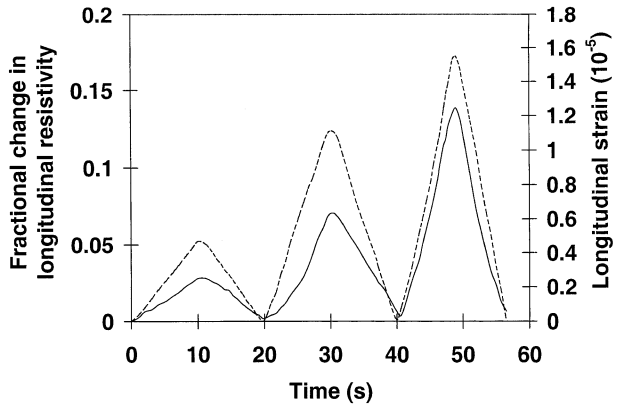

Fig. 2. Variation of the fractional change in longitudinal electrical resistivity with time (solid curve) and of the strain with time (dashed curve) during dynamic uniaxial tensile loading at increasing stress amplitudes within the elastic regime for cement paste (iii).

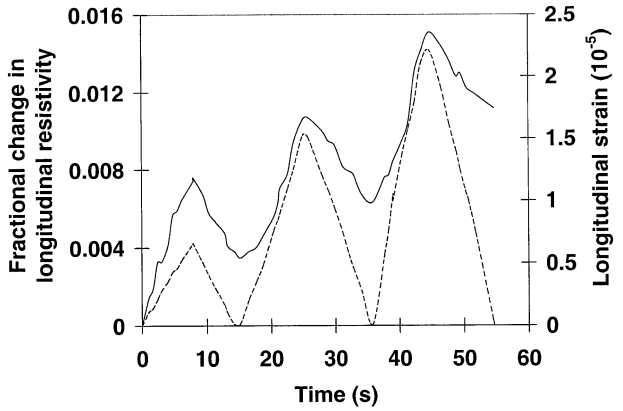

Fig. 4. Variation of the fractional change in longitudinal electrical resistivity with time (solid curve) and of the strain with time (dashed curve) during dynamic uniaxial tensile loading at increasing amplitudes within the elastic regime for cement paste (ii).

For measuring the longitudinal resistance, the electrical contacts were made by silver paint applied along the whole perimeter in four parallel planes perpendicular to the stress axis, as illustrated in Fig. 1(b). For measuring the transverse resistance, two electrical contacts in the form of lines parallel to the stress axis were made by silver paint applied on each of two opposite sides of the specimen parallel to the stress axis, such that one contact on each side was electrically connected by copper wire to the nearby contact on the opposite side (Fig. 1(b)); the other two electrical contacts were made by applying silver paint on each of the two remaining surfaces parallel to the stress axis (Fig. 1(b)). In both longitudinal and transverse cases, the inner two contacts were for voltage measurement, while the outer two contacts were for passing a current. The longitudinal and transverse strains and the longitudinal and transverse resistances were simultaneously measured for each specimen. A Keithley (Keithley Instruments, Cleveland, OH) 2001 multimeter was used. For the longitudinal resistance measurement, the outer two contacts were typically 80 mm apart and the inner two contacts were typically 70 mm apart; for the transverse resistance measurement, the outer two contacts were typically 30 mm apart and the inner two contacts were typically 20 mm apart. Although the spacing between the contacts changed upon deformation, the change was so small that the measured resistance remained essentially proportional to the volume resistivity.

3. Results and discussion

Figs. 2 and 3 show the fractional changes in the longitudinal and transverse resistivities, respectively for cement paste (iii) during repeated unaxial tensile loading at increasing strain amplitudes. The strain essentially returned to zero at the end of each cycle, indicating elastic deformation. The longitudinal strain was positive (i.e., elongation); the transverse strain was negative (i.e., shrinkage due to the Poisson effect). Both longitudinal and transverse resistivities increased reversibly upon uniaxial tension. The

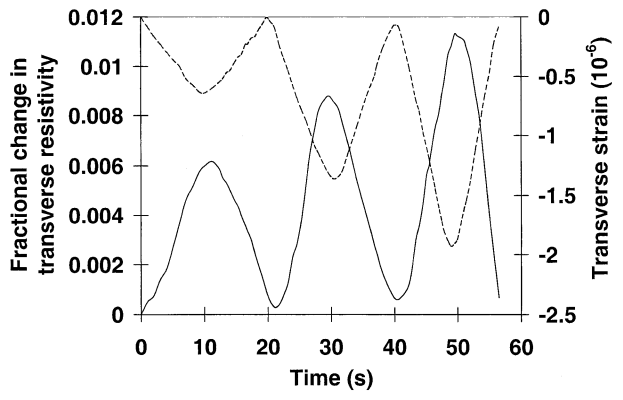

Fig. 3. Variation of the fractional change in transverse electrical resistivity with time (solid curve) and of the strain with time (dashed curve) during dynamic uniaxial tensile loading at increasing amplitudes within the elastic regime for cement paste (iii).

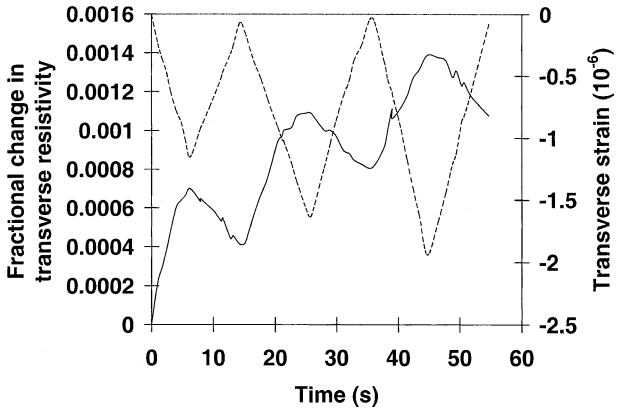

Fig. 5. Variation of the fractional change in transverse electrical resistivity with time (solid curve) and of the strain with time (dashed curve) during dynamic uniaxial tensile loading at increasing amplitudes within the elastic regime for cement paste (ii).

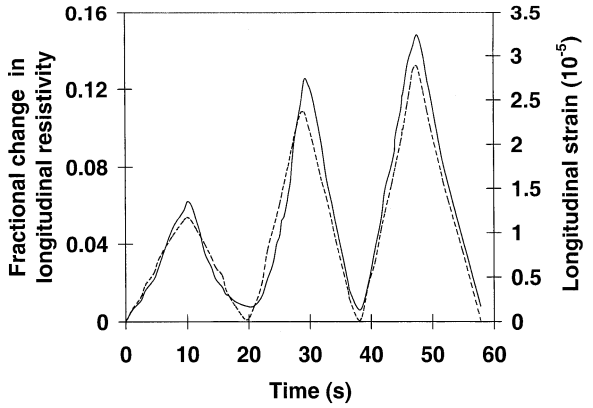

Fig. 6. Variation of the fractional change in longitudinal electrical resistivity with time (solid curve) and of the strain with time (dashed curve) during dynamic uniaxial tensile loading at increasing amplitudes within the elastic regime for cement paste (v).

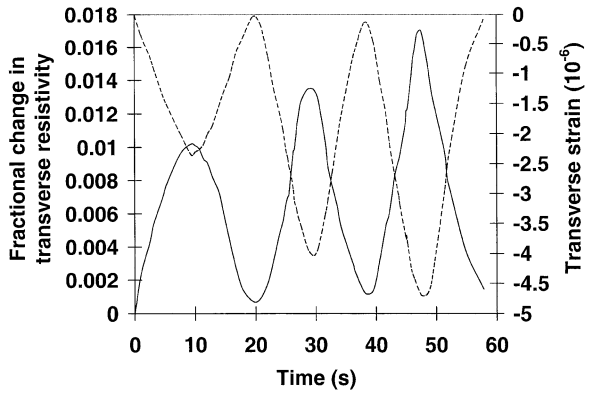

Fig. 7. Variation of the fractional change in transverse electrical resistivity with time (solid curve) and of the strain with time (dashed curve) during dynamic uniaxial tensile loading at increasing amplitudes within the elastic regime for cement paste (v).

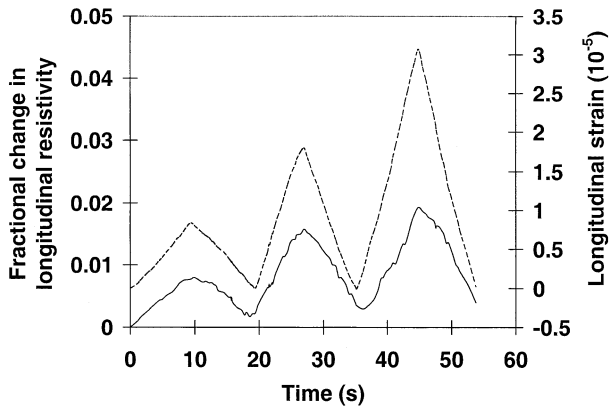

Fig. 8. Variation of the fractional change in longitudinal electrical resistivity with time (solid curve) and of the strain with time (dashed curve) during dynamic uniaxial tensile loading at increasing amplitudes within the elastic regime for cement paste (iv).

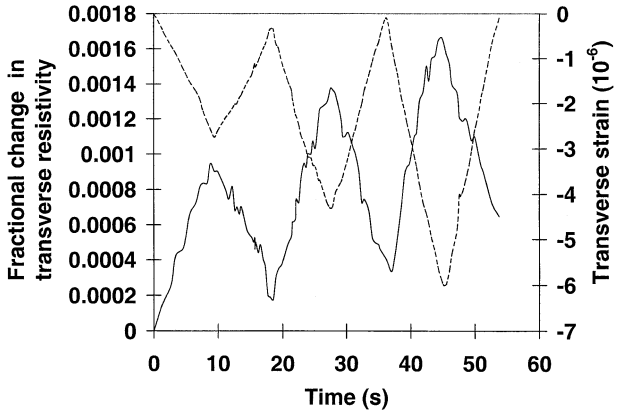

Fig. 9. Variation of the fractional change in transverse electrical resistivity with time (solid curve) and of the strain with time (dashed curve) during dynamic uniaxial tensile loading at increasing amplitudes within the elastic regime for cement paste (iv).

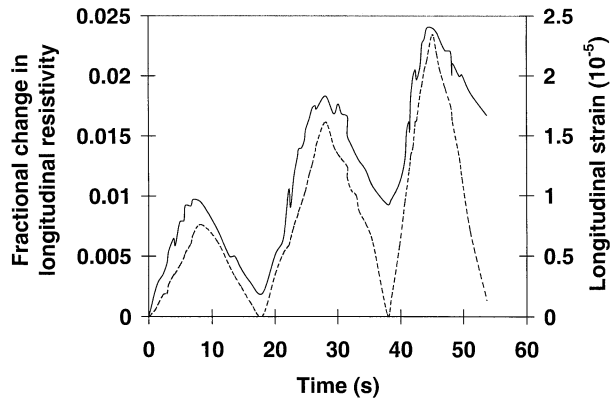

Fig. 10. Variation of the fractional change in longitudinal electrical resistivity with time (solid curve) and of the strain with time (dashed curve) during dynamic uniaxial tensile loading at increasing amplitudes within the elastic regime for cement paste (i).

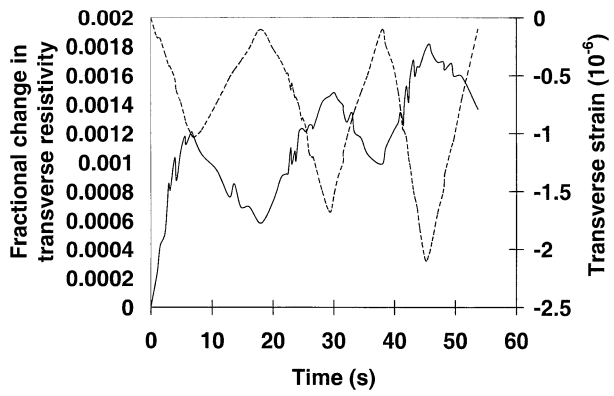

Fig. 11. Variation of the fractional change in transverse electrical resistivity with time (solid curve) and of the strain with time (dashed curve) during dynamic uniaxial tensile loading at increasing amplitudes within the elastic regime for cement paste (i).

reversibility of both strain and resistance was more complete in the longitudinal direction than the transverse direction. The gage factor (i.e., fractional change in resistance per unit strain in the same direction, essentially the same as the fractional change in resistivity per unit strain) was 89 and −59 for the longitudinal and transverse resistances, respectively.

Figs. 4 and 5 show corresponding results for cement paste (ii). The strain was essentially totally reversible in both the longitudinal and transverse directions, but the resistivity was only partly reversible in both directions, in contrast to the reversibility of the resistivity when fibers were present (Figs. 2 and 3). As in the case with fibers (Figs. 2 and 3), both longitudinal and transverse resistivities increased upon uniaxial tension. However, the gage factor was only 7.2 and −7.1 for Figs. 4 and 5, respectively.

Cement pastes (ii) and (iii) were identical except that paste (ii) had no fibers whereas paste (iii) had fibers. Comparison of Figs. 2 and 3 (paste (iii)) with Figs. 4 and 5 (paste (ii)) shows that fibers greatly enhanced the magnitude and reversibility of the resistivity effect. The gage factors were much smaller in magnitude when fibers were absent.

Figs. 6 and 7 show corresponding results for cement paste (v). The behavior was similar to that of cement paste (iii), as both pastes (v) and (iii) had fibers. The gage factors were 51 and −36 in the longitudinal and transverse directions, respectively, for paste (v). These values are smaller in magnitude than those for paste (iii), as expected from the higher resistivity for paste (v) than paste (iii) [13].

Figs. 8 and 9 show corresponding results for cement paste (iv). The behavior was similar to that of cement paste (ii), as both pastes (iv) and (ii) had no fiber. The gage factors were 6.3 and −2.8 in the longitudinal and transverse directions, respectively, for paste (iv).

Figs. 10 and 11 show corresponding results for cement paste (i). The behavior was similar to that of cement pastes (ii) and (iv), as pastes (i), (ii) and (iv) had no fiber. The gage factors were 10 and −8.7 in the longitudinal and transverse directions, respectively, for paste (i).

The increase in both longitudinal and transverse resistivities upon uniaxial tension for all pastes, whether with or without fibers, is attributed to defect (e.g., microcrack) generation. In the presence of fibers, fiber bridging across microcracks occurs and slight fiber pull-out occurs upon tension, thus enhancing the possibility of microcrack closing and causing more reversibility in the resistivity change. The fibers are much more electrically conductive than the cement matrix. The presence of the fibers introduces interfaces between fibers and matrix. The degradation of the fiber–matrix interface due to fiber pull-out or other mechanisms is an additional type of defect generation which will increase the resistivity of the composite. Therefore, the presence of fibers greatly increases the gage factor.

The transverse resistivity increases upon uniaxial tension, even though the Poisson effect causes the transverse strain to be negative. This means that the effect of the transverse resistivity increase overshadows the effect of the transverse shrinkage. The resistivity increase is a consequence of the uniaxial tension. In contrast, under uniaxial compression, the resistance in the stress direction decreases at 28 days of curing [6–11], as explained in Section 1. Hence, the effects of uniaxial tension on the transverse resistivity and of uniaxial compression on the longitudinal resistivity are different; the gage factors are negative and positive for these cases, respectively.

The similarity of the resistivity change in longitudinal and transverse directions under uniaxial tension suggests similarity for other directions as well. This means that the resistance can be measured in any direction in order to sense the occurrence of tensile loading. Although the gage factor is comparable in both longitudinal and transverse directions, the fractional change in resistance under uniaxial tension is much higher in the longitudinal direction than the transverse direction. Thus, the use of the longitudinal resistance for practical self-sensing is preferred.

4. Conclusion

Uniaxial tension of carbon fiber reinforced cement in the elastic regime was found to cause reversible increases in both longitudinal and transverse resistivities, such that the gage factor was comparable in magnitude in the two directions. In contrast, uniaxial compression causes reversible decrease in the longitudinal resistivity, as previously reported [6–11]. Without the fibers, the resistivity increase under uniaxial tension was much smaller and less reversible. The resistivity increase is attributed to defect generation under tension.

Acknowledgments

This work was supported by the National Science Foundation, USA

References

[1] P.-W. Chen, D.D.L. Chung, Concrete reinforced concrete as a smart material capable of non-destructive flaw detection, Smart Mater Struct 2 (1993) 22–30.
[2] P.-W. Chen, D.D.L. Chung, Concrete as a new strain/stress sensor, Composites Part B 27B (1996) 11–23.
[3] P.-W. Chen, D.D.L. Chung, Carbon fiber reinforced concrete as an intrinsically smart concrete for damage assessment during dynamic loading, J Am Ceram Soc 78 (3) (1995) 816–818.
[4] D.D.L. Chung, Strain sensors based on the electrical resistance change accompanying the reversible pull-out of conducting short fibers in a less conducting matrix, Smart Mater Struct 4 (1995) 59–61.
[5] P.-W. Chen, D.D.L. Chung, Carbon fiber reinforced concrete as an

intrinsically smart concrete for damage assessment during static and dynamic loading, ACI Mater J 93 (4) (1996) 341–350.
[6] X. Fu, D.D.L. Chung, Self-monitoring of fatigue damage in carbon fiber reinforced cement, Cem Concr Res 26 (1) (1996) 15–20.
[7] X. Fu, E. Ma, D.D.L. Chung, W.A. Anderson, Self-monitoring in carbon fiber reinforced mortar by reactance measurement, Cem Concr Res 27 (6) (1997) 845–852.
[8] X. Fu, D.D.L. Chung, Effect of curing age on the self-monitoring behavior of carbon fiber reinforced mortar, Cem Concr Res 27 (9) (1997) 1313–1318.
[9] X. Fu, W. Lu, D.D.L. Chung, Improving the strain sensing ability of carbon fiber reinforced cement by ozone treatment of the fibers, Cem Concr Res 28 (2) (1998) 183–187.
[10] X. Fu, W. Lu, D.D.L. Chung, Ozone treatment of carbon fiber for reinforcing cement, Carbon 36 (9) (1998) 1337–1345.
[11] M. Qizhao, Z. Binyuan, S. Darong, L. Zhuoqiu, Resistance changement of compression sensible cement specimen under different stresses, J Wuhan Univ Technol 11 (3) (1996) 41–45.
[12] Z.-Q. Shi, D.D.L. Chung, Carbon fiber reinforced concrete for traffic monitoring and weighing in motion, Cem Concr Res 29 (3) (1999) 435–439.
[13] P.-W. Chen, X. Fu, D.D.L. Chung, Microstructural and mechanical effects of latex, methylcellulose and silica fume on carbon fiber reinforced cement, ACI Mater J 94 (2) (1997) 147–155.